

Impacts of urban and cropland expansions on natural habitats in Southeast Asia

Received: 9 June 2024

Accepted: 15 August 2025

Published online: 26 September 2025

 Check for updatesXinmin Zhang¹✉, Wenqiang Wan¹ & Ronald C. Estoque²

Urban and cropland expansions greatly contribute to natural habitat loss. Few studies have focused on the direct and indirect impacts of urban and cropland expansions on natural habitats in Southeast Asia, a biodiversity hotspot. In this study, these impacts were quantified from 2000 to 2020 across three scales (country, ecoregion, and biome) and future Shared Socioeconomic Pathways (SSPs) (by 2030 and 2050). From 2000 to 2020, the impact of cropland expansion on natural habitats in Southeast Asia was nearly 16 times greater than that of urban expansion. The impact of cropland expansion was primarily direct, whereas the indirect impact of urban expansion was approximately 14 times greater than the direct impact during the same period. Under the 2050 SSP3 (regional rivalry scenario), the projected areas of cropland expansion reaches $113.19 \times 10^3 \text{ km}^2$, resulting in the most pronounced impact on natural habitats. Under future SSPs, the gap between the total impacts of cropland and urban expansions, as well as the gap between the indirect and direct impacts of urban expansion, is expected to narrow compared with current conditions. Our study suggests that natural habitat conservation efforts in Southeast Asia should address the varying impacts of urban and cropland expansions through aspects such as urban form, spatial planning, and agricultural structure.

Land use and cover (LUC) changes have accelerated the reorganization of terrestrial ecosystems¹, with both urban expansion and cropland expansion acting as major drivers of biodiversity loss^{1–3}. Urban expansion encroaches on natural habitats, resulting in substantial reductions in biodiversity². Cropland expansion, driven by the demand for food, is a leading threat to biodiversity^{4,5}. Southeast Asia, which encompasses at least four global biodiversity hotspots and 15% of the global tropical forests^{6–8}, is particularly vulnerable to the impacts of both urban expansion and cropland expansion. Large-scale anthropogenic activities associated with urban expansion have accelerated forest loss in Southeast Asia^{1,9}, leading to severe habitat destruction and biodiversity loss^{6,7}. Additionally, the expansion of both highland and lowland cropland areas in Southeast Asia has contributed to the formation of deforestation hotspots¹. The expansion of $27.0 \times 10^4 \text{ km}^2$ of cropland led to extensive forest loss between 2000 and 2014¹⁰, making Southeast Asia as one of the regions where biodiversity is most threatened by agricultural production¹. Therefore, assessing the

impacts of urban and cropland expansions on natural habitats is important for biodiversity conservation.

Natural habitats are subject to both direct and indirect impacts resulting from urban and cropland expansions. Urban and cropland expansions directly affect natural habitats, mainly through habitat loss in forested areas^{3,10,11}. Additionally, urban and cropland expansions indirectly affect surrounding natural habitats through trampling and nonpoint source disturbances^{3,10,12,13}, such as runoff, water, and air pollution, which cannot be attributed to a specific source or location. Studies have assessed the impacts of urban and cropland expansions on natural habitats^{3,10,14,15}. Between 1985 and 2015, an estimated 12% and 9% of global urban expansion occurred at the expense of grasslands and forestlands, respectively^{3,14}. Similarly, the global cropland area increased by 9% from 2003 to 2019, with nearly 50% of this new cropland area displacing natural habitats; moreover, global cropland is projected to expand by 26% from 2010 to 2050^{10,15}, coinciding with an anticipated increase in global population from 8.5 to 9.9 billion². This

¹School of Digital Economics, Jiangxi University of Finance and Economics, Nanchang, China. ²Center for Biodiversity and Climate Change, Forestry and Forest Products Research Institute, Tsukuba, Japan. ✉e-mail: zhangxm1217@aliyun.com

growth will substantially increase the demand for urban land, intensifying pressure on the conservation of natural habitats and biodiversity.

Research in Southeast Asia has focused primarily on assessing the preservation status of natural habitats by examining specific species or the impacts of climate change^{16–18}. Many studies have measured the direct impacts of urban and cropland expansions on natural habitats, but they often overlook indirect impacts. In Southeast Asia, urban and cropland expansions strongly contribute to natural habitat loss and threaten biodiversity^{4,5,19}. The substantial indirect impacts of urban and cropland expansions on natural habitats are frequently neglected. Furthermore, the impacts of urban and cropland expansions across various future scenarios have not been sufficiently studied. A global study of drylands revealed that the indirect impact of urban expansion, which decreases habitat quality, is 10 to 15 times greater than the direct impact³. Therefore, quantifying both the direct and indirect impacts of urban and cropland expansions on natural habitats is urgently needed and holds notable scientific importance. The habitat quality index (HQI) reflects the capacity of habitats to support the survival and development of species³. It can be used to effectively assess the direct and indirect impacts of urban and cropland expansions on natural habitats^{3,10,20}, and demonstrates good results in different types of regions. Therefore, the HQI was used as an indicator in this research, aiming to comprehensively assess the direct and indirect impacts of urban and cropland expansions in Southeast Asia.

The objective of this study is to reveal the dynamics of urban and cropland expansions in Southeast Asia and assess the direct and indirect impacts of these expansions on natural habitats. Specifically, we followed the parameter framework for evaluating the HQI in drylands proposed by Ren et al.³, and generated the HQI using InVEST model^{21,22}. Then, we assessed the direct and indirect impacts of urban and cropland expansions on natural habitats in Southeast Asia from 2000 to 2020 at the country, ecoregion, and biome scales (Supplementary Figs. 1 and 2). In this study, the decrease in the HQI resulting from the direct encroachment of urban and cropland areas into natural habitats was defined as the direct impact; whereas the encroachment of urban and cropland expansions into non-natural habitats, and the decrease in the HQI within the maximum influence distances of urban and cropland areas was used to determine the indirect impact. Additionally, by constructing a linear regression model, we determined the demands for urban land in 2030 and 2050 under various Shared Socioeconomic Pathways (SSPs). Subsequently, we utilized the PLUS model to simulate future LUC patterns. Then, we assessed the direct and indirect impacts of urban and cropland expansions on natural habitats in Southeast Asia under the various SSPs.

Results

Natural habitat loss, and the dynamics of urban and cropland expansions

Between 2000 and 2020, the natural habitat area in Southeast Asia decreased by 3.07%, from $282.70 \times 10^4 \text{ km}^2$ (59.80% of the total land area) to $274.03 \times 10^4 \text{ km}^2$ (57.96%), showing a continuous downward trend (Fig. 1). Urban areas increased from $19.12 \times 10^3 \text{ km}^2$ in 2000 to $36.01 \times 10^3 \text{ km}^2$ in 2020, with 91.95% of this expansion occurring at the expense of croplands and an expansion rate of 3.22% (Fig. 2). Cropland expansion far exceeded urban expansion in terms of area, increasing from $186.21 \times 10^4 \text{ km}^2$ to $192.64 \times 10^4 \text{ km}^2$, with an expansion rate of 0.17%, while approximately 89% of the total cropland expansion was converted from forestland. In addition, the increase in urban expansion from 2000 to 2010 (7121.88 km^2) was less than that from 2010 to 2020 (9814.41 km^2), whereas the opposite change was observed for cropland expansion (2000–2010: $46.73 \times 10^3 \text{ km}^2$; 2010–2020: $17.62 \times 10^3 \text{ km}^2$).

During the 2000–2020 period, the natural habitat area decreased in seven countries (Fig. 1b). Indonesia exhibited the greatest reduction, with a decrease of $63.09 \times 10^3 \text{ km}^2$ (Supplementary Table 1), representing 72.78% of the total loss in Southeast Asia. Correspondingly, its

urban and cropland expansion areas were the largest among all countries (Supplementary Fig. 3), expanding by 5857.65 km^2 (with an expansion rate of 2.00%) and $52.12 \times 10^3 \text{ km}^2$ (0.38%), respectively (Supplementary Tables 2 and 3). In addition, there was modest expansion in the natural habitat areas of Thailand, the Philippines, Brunei, and Timor-Leste, with increases in the natural habitat area accounting for 0.28%, 0.50%, 1.23%, and 0.62% of their country areas, respectively (Supplementary Table 1).

The largest loss in the natural habitat area was observed in the other ecoregions (OER), totaling $5.96 \times 10^4 \text{ km}^2$ and the largest area of urban and cropland expansions was also exhibited in the OER (Supplementary Table 1, Supplementary Fig. 4), with the urban area increasing from $16.91 \times 10^3 \text{ km}^2$ in 2000 to $30.57 \times 10^3 \text{ km}^2$ in 2020 (3.00%) and the area of cropland expansion covering $41.51 \times 10^3 \text{ km}^2$ (0.18%) (Supplementary Tables 2 and 3). This growth signifies that the percentage of cropland in the OER has slightly increased from 61.14% to 61.25% across Southeast Asia.

From 2000 to 2020, natural habitat areas decreased in six biomes (Fig. 1b). Tropical and subtropical moist broadleaf forests (TSMBF), exhibited the greatest decrease in natural habitats across Southeast Asia, with a reduction of 3.20%, totaling $79.42 \times 10^3 \text{ km}^2$ (Supplementary Table 1). Moreover, TSMBF exhibited the largest area of urban expansion (Supplementary Fig. 5), reaching $13.26 \times 10^3 \text{ km}^2$, which exceeded the urban expansion area of the other biomes (Fig. 2, Supplementary Table 2). The cropland expansion area of TSMBF was $61.01 \times 10^3 \text{ km}^2$ (0.22%) (Supplementary Table 3), approximately 20 times the total cropland expansion area of the other seven biomes. These changes are likely related to its geographical range, as the TSMBF constitutes 83.21% of the total land area in Southeast Asia (Supplementary Fig. 2).

Direct and indirect impacts on natural habitats

The indirect impact of urban expansion on natural habitats in Southeast Asia substantially surpassed the direct impact; conversely, the direct impact of cropland expansion exceeded its indirect impact. Overall, influenced by urban expansion, the mean HQI in Southeast Asia experienced a decline of 0.35% (Fig. 3a). The direct impact of urban expansion on natural habitats reached 0.024%, which suggests that the area directly affected was 1052.91 km^2 . The area indirectly affected by urban expansion reached $15.88 \times 10^3 \text{ km}^2$, with an indirect impact of 0.326%, which was 13.76 times greater than the direct impact. The impact of cropland expansion on natural habitats in Southeast Asia differed from that of urban expansion. Overall, cropland expansion generated substantial direct impacts across all scales, while its corresponding indirect impacts were generally lower (Fig. 3b). The total impact of cropland expansion reached 5.699%, and the direct impact of cropland expansion was dominant.

The indirect impacts of urban expansion exceeded the direct impacts in all countries. Indonesia was the most affected by urban and cropland expansions, with a direct impact of approximately 0.010% from urban expansion and an indirect impact of 0.094%, which was 9.52 times greater than the direct impact (Fig. 3b and Supplementary Table 2). Approximately 89% of cropland expansion in Southeast Asia was from deforestation, which explained the greater direct impact of cropland expansion. As Indonesia has the largest area of cropland expansion in Southeast Asia, it exhibited the greatest direct impact of cropland expansion (3.500%). In terms of indirect impact, only Indonesia, Cambodia, and Vietnam were affected (Supplementary Table 3).

Across various ecoregions, the impacts of urban and cropland expansions mostly affected the OER and lowland rainforest ecoregions (Fig. 3b). Specifically, the indirect impacts due to urban expansion in the OER, Borneo lowland rainforests (BLRF), and Sumatra lowland rainforests (SLRF) reached 0.221%, 0.019%, and 0.018%, respectively, which were 12.47, 6.95, and 24.55 times of the corresponding direct impacts, respectively (Fig. 3b and Supplementary Table 2). Since there

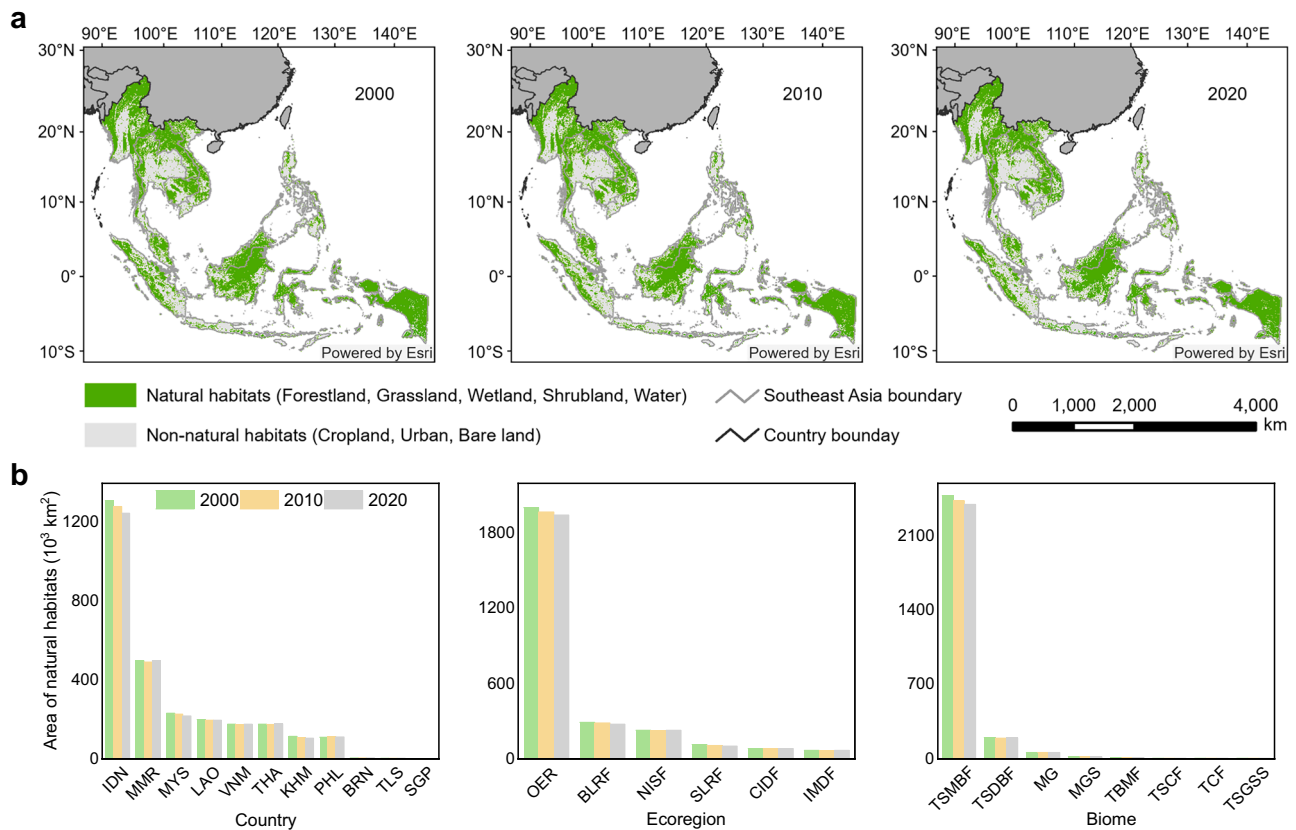


Fig. 1 | Spatial distribution of natural habitats in Southeast Asia during 2000–2020 (references to the ESA LUC data sources are provided in the “Methods” and “Data availability” sections, and the national administrative boundaries were derived from the Global Administrative Areas: www.gadm.org). **a Spatial distribution of natural habitats; and **b** corresponding area statistics, the bars represent the area of natural habitats. BRN Brunei, IDN Indonesia, KHM Cambodia, LAO Laos, MYS Malaysia, MMR Myanmar, PHL Philippines, SGP Singapore, THA Thailand, TLS Timor-Leste, VNM Vietnam, BLRF Borneo lowland**

rainforests, CIDF Central Indochina dry forests, NISF Northern Indochina subtropical forests, SLRF Sumatran lowland rainforests, IMDF Irrawaddy moist deciduous forests, OER other ecoregions, TSMBF tropical and subtropical moist broadleaf forests, TSDBF tropical and subtropical dry broadleaf forests, MG Mangroves, MGS Montane grasslands and shrublands, TBMF temperate broadleaf and mixed forests, TSCF tropical and subtropical coniferous forests, TCGSS tropical and subtropical grasslands, savannas and shrublands, TCF temperate conifer forests.

was no urban expansion in temperate broadleaf and mixed forests (TBMF) and temperate coniferous forests (TCF), the corresponding direct and indirect impacts were 0. In all ecoregions, the indirect impact of cropland expansion did not exceed 0.001%, and the OER, BLRF, and SLRF were strongly affected by the direct impact of cropland expansion, with direct impacts of 3.630%, 1.016%, and 0.746%, respectively (Fig. 3b and Supplementary Table 3).

The impacts of urban and cropland expansions were concentrated in broadleaf forest biomes, mainly in the TSMBF (Fig. 3b). The direct impact of urban expansion in the TSMBF reached 0.018%, whereas the indirect impact was 13.96 times greater than the direct impact (Supplementary Table 2). As TSMBF is highly dominant in Southeast Asia, 95.16% of cropland expansion in the region occurred in the TSMBF, which resulted in a combined direct and indirect impact of 5.116% (Supplementary Table 3), surpassing the values of other biomes. In addition to the TSMBF, other broadleaf and mangrove biomes, such as tropical and subtropical dry broadleaf forests (TSDBF) and mangroves (MG), also experienced greater direct impacts (0.408% and 0.131%, respectively) (Fig. 3b and Supplementary Table 3).

Future expansion and its impacts on natural habitats in 2030 and 2050

Urban expansion and cropland expansion exhibited distinct differences in future scenarios. SSP5 (fossil-fueled development scenario) exhibits the greatest urban expansion and the smallest extent of cropland expansion, whereas the SSP3 scenario results in the greatest

cropland expansion and the smallest extent of urban expansion (Fig. 4). In the 2050 SSP5 scenario, the projected urban expansion area reached $90.14 \times 10^3 \text{ km}^2$, with the highest expansion rate of 3.55%, leading to the greatest natural habitat loss, totaling $197.59 \times 10^3 \text{ km}^2$ (Fig. 4a). Concurrently, the indirect impacts of urban expansion are projected to exceed the direct impacts across all the scenarios. Specifically, the indirect impact under the 2030 SSP1 (sustainability scenario) will be 5.30 times greater than the direct impact, and this value will decrease to 1.03 times under the 2050 SSP5 scenario (Fig. 5a). For cropland expansion, the 2050 SSP3 scenario shows the highest increase, with a cropland expansion area of $113.19 \times 10^3 \text{ km}^2$. In all the scenarios, the direct impacts of cropland expansion far exceeded the indirect impacts, and the gap increases over time (Fig. 5b).

The direct impacts of urban expansion in countries were observed to exceed the indirect impacts. Indonesia, Thailand, Vietnam, and Malaysia will continue to experience rapid urban expansion in 2030 and 2050 under SSP1 and SSP5 scenarios (Fig. 4b, Supplementary Tables 4 and 5). Among them, the urban expansion of Indonesia peaks in the 2050 SSP5 scenario, with the urban expansion area reaching $53.56 \times 10^3 \text{ km}^2$, causing its direct impact (1.908%) that surpasses the indirect impact (1.055%) (Fig. 5a, Supplementary Tables 6 and 7). In contrast, under the 2050 SSP3 scenario, the impact of cropland expansion will be the greatest. Indonesia, which is projected to experience the largest cropland expansion (Supplementary Tables 8 and 9), will present the greatest direct impact (4.374%) under the 2050 SSP3 scenario (Fig. 5b, Supplementary Tables 10 and 11).

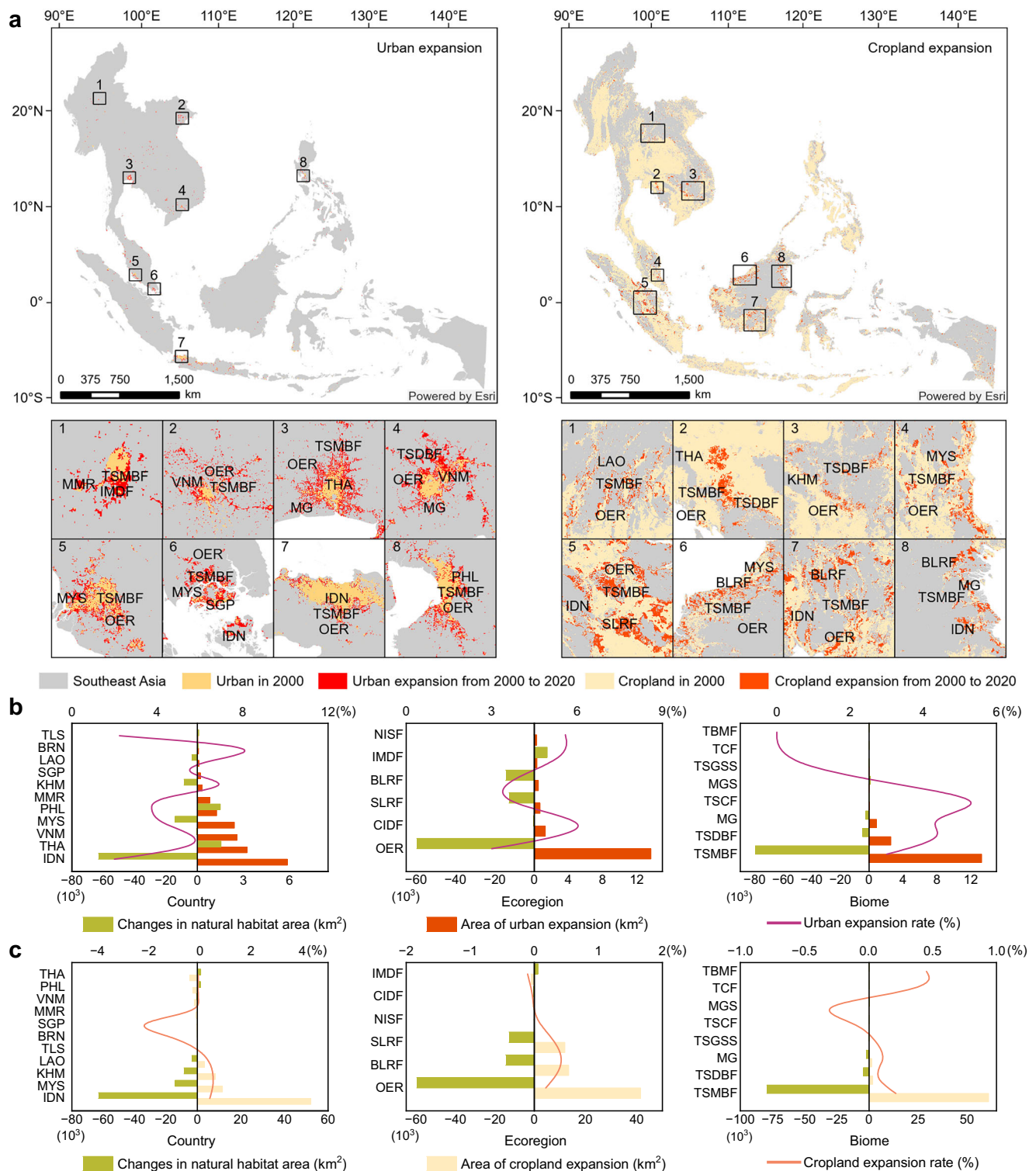


Fig. 2 | Urban expansion and cropland expansion during 2000–2020 (the national administrative boundaries were derived from the Global Administrative Areas: www.gadm.org). a Spatial distributions of urban and cropland expansions, with rectangular boxes indicating representative areas of urban and

cropland expansions; **(b)** urban expansion area, expansion rate, and changes in the natural habitat area; and **(c)** cropland expansion area, expansion rate, and changes in the natural habitat area.

Among six ecoregions, the OER and lowland rainforest ecoregions are projected to experience continued trends of urban and cropland expansions (Fig. 4b, c). The urban expansion area in the OER is projected to reach $75.64 \times 10^3 \text{ km}^2$ in the 2050 SSP5 scenario (Supplementary Table 5). Furthermore, the OER has indirect impacts that are lower than the direct impacts under the 2050 SSP1 and 2050

SSP5 scenarios (Fig. 5a, Supplementary Table 7). In contrast, OER, BLRF, and SLRF exhibit pronounced cropland expansion in 2030 and 2050 under SSP2 (middle of the road scenario), SSP3, and SSP4 (inequality scenario), respectively (Supplementary Tables 8 and 9). The direct impacts of cropland expansion are projected to increase across all ecoregions (particularly in the SSP3 scenario), whereas the

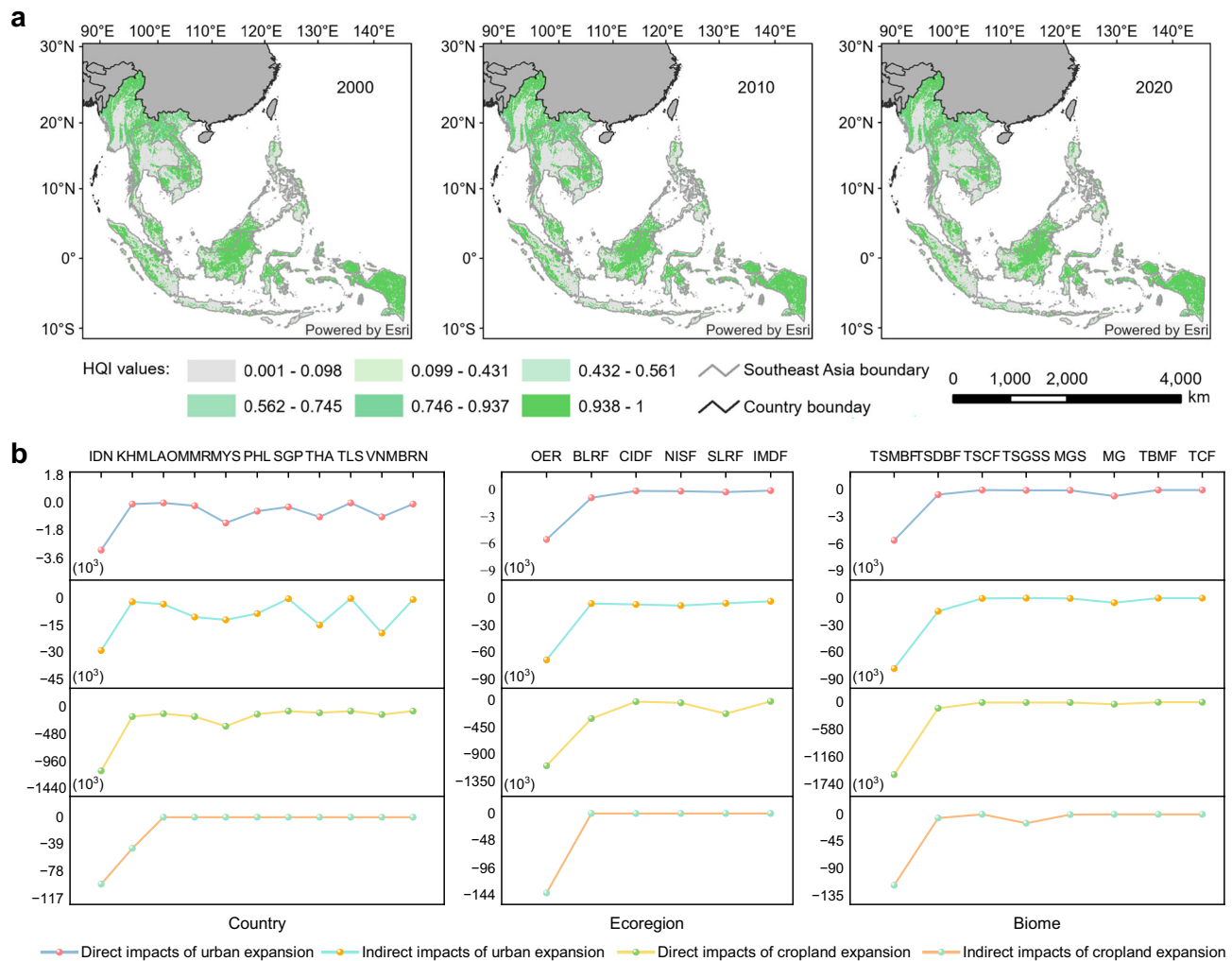


Fig. 3 | Direct and indirect impacts of urban and cropland expansions during 2000–2020 (the national administrative boundaries were derived from the Global Administrative Areas: www.gadm.org). a Spatial distribution of the HQI; and **(b)** direct and indirect impacts of urban and cropland expansions.

changes in indirect impacts are not as pronounced (Fig. 5b, Supplementary Tables 10 and 11).

Broadleaf forests and mangrove biomes will be more substantially affected by urban and cropland expansions in 2030 and 2050 (Fig. 4b, c). Specifically, urban expansion could continue in the TSMBF, TSDBF, and MG, with the urban expansion areas increasing under the SSP1 and SSP5 scenarios in 2030 and 2050. Particularly, the TSMBF could experience the greatest expansion ($76.32 \times 10^3 \text{ km}^2$) under the 2050 SSP5 scenario (Supplementary Table 5), resulting in substantial total impacts (4.831%) (Fig. 5a, Supplementary Table 7). For cropland expansion, there are notable increases in the TSMBF and TSDBF under the SSP3 scenario in 2030 and 2050. Although the increases in other scenarios may be less substantial, they could still lead to a combined expansion area of the TSMBF and TSDBF that exceeds the total increase in all other biomes (Supplementary Tables 8 and 9). This results in the greatest direct impacts for TSMBF (6.658%) and TSDBF (0.584%) in the 2050 SSP3 scenario, whereas the direct impacts in other biomes gradually increase to lesser levels (Fig. 5b, Supplementary Tables 10 and 11).

Impacts of urban and cropland expansions on threatened species

The focus of this study was on assessing the indirect impact of urban expansion and the direct impact of cropland expansion on threatened species. The highest species richness value in Southeast Asia was 901,

of which the highest species richness value of threatened species was 90. On average, there were approximately 43 threatened species per pixel, and the rarity-weighted richness patterns of all species and threatened species were highly consistent. The areas of relatively high importance for species were distributed mainly in coastal regions and islands (Fig. 6a).

Since there are no distinct changes in the average value of affected threatened species in the 2030 and 2050 scenarios, we focus on the average value of affected threatened species caused by urban and cropland expansions during 2000–2020 and under all future scenarios. We found that both urban expansion and cropland expansion most prominently affected threatened bird species, followed by mammals and amphibians. Urban expansion indirectly affected 17.63 threatened birds and 14.85 threatened mammals, whereas cropland expansion directly affected 19.06 and 18.26 species of these types, respectively (Fig. 6b).

Among all scales, Brunei experienced the greatest impacts on threatened birds and mammals, with more than 34 species affected by urban and cropland expansions on average (Fig. 6b). Additionally, there are scale differences in the impacts of urban and cropland expansions on threatened birds and mammals. Indonesia, Malaysia, and Singapore exhibited the highest average values of affected threatened bird and mammal species. The two lowland rainforest ecoregions, i.e., BLRF and SLRF, were associated with the most severe impacts on threatened birds and mammals among all ecoregions.

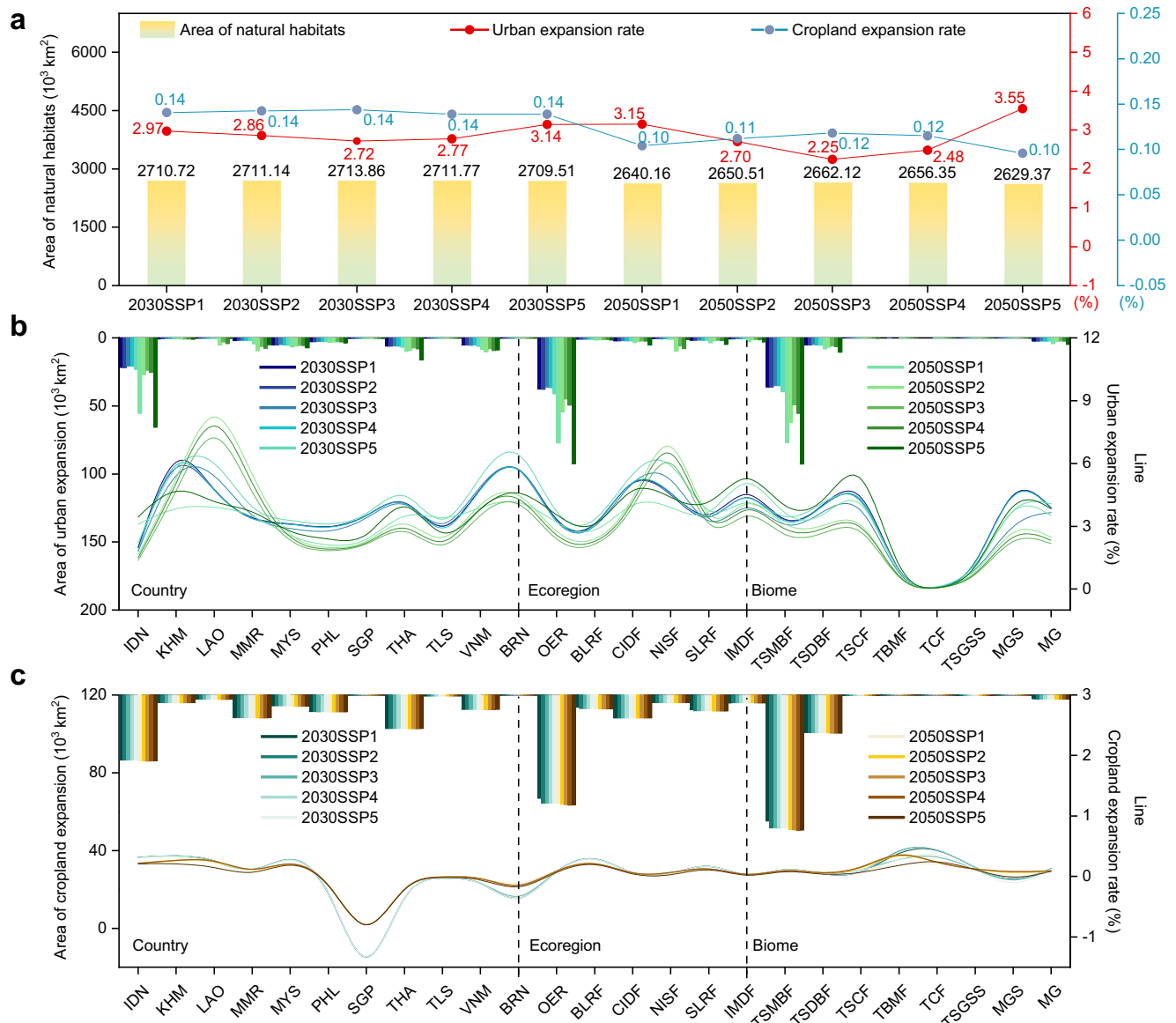


Fig. 4 | Urban and cropland expansions in 2030 and 2050 under the various SSPs. a Total areas of natural habitats, urban expansion rate and cropland expansions rate; **(b)** urban expansion area and the expansion rates at three scales; and **(c)** cropland expansion area and the expansion rates at three scales. The bars in **(a, b)** represent the expansion areas, and the lines represent the expansion rates.

Among the biomes, MGS exhibited the highest average values of affected threatened birds and mammals under the indirect impacts of urban expansion, with 22.51 and 29.18 species, respectively (Fig. 6b). Under the direct impacts of cropland expansion, MG showed the greatest average values of affected threatened birds and mammals, with 26.65 and 20.26 species, respectively (Fig. 6b).

Discussion

Urban expansion and cropland expansion are the primary drivers behind the biodiversity decline in Southeast Asia^{4,5,19}. In this study, we found that the urban expansion area during 2000–2010 was less than that during 2010–2020, whereas cropland expansion occurred more during 2000–2010. This phenomenon was due to the competitive interaction between urban land and cropland, and the stage differences in urbanization and agricultural transformation in Southeast Asia. Following the S-curve of urbanization, the process of urbanization can be categorized into three stages (initial stage; acceleration stage, i.e., 30–70%; and terminal stage), and Southeast Asia is currently in the acceleration stage²³. Southeast Asia surpassed an urbanization

rate of 30% in 1995, and by 2015, the rate had nearly reached 48%²⁴. With the acceleration of urbanization, the demand for urban land rapidly increased from 2010 to 2020. Concurrently, the transformation of the traditional agricultural system in Southeast Asia from extensive agriculture to intensive agriculture has increased the yield of cropland²⁵, reduced the need for new land reclamation, and may have also slowed cropland expansion.

Although urban expansion primarily occurred through encroachment on cropland, and cropland expansion mainly occurred via the destruction of forests in Southeast Asia, some regions were still affected by both urban expansion and cropland expansion across three scales. Indonesia is the country most notably affected by urban and cropland expansions. As the largest country in Southeast Asia, Indonesia requires substantial amounts of urban land and food to support its population (216 million in 2000 to 275 million in 2020). In addition, Indonesia is the leading global producer of palm oil²⁶, and together with Malaysia, they contribute to 81.90% of the global oil palm fruit output, with a remarkable increase of 179.72% from 2000 to 2017²⁷. This dramatic expansion of oil palm fields has resulted in

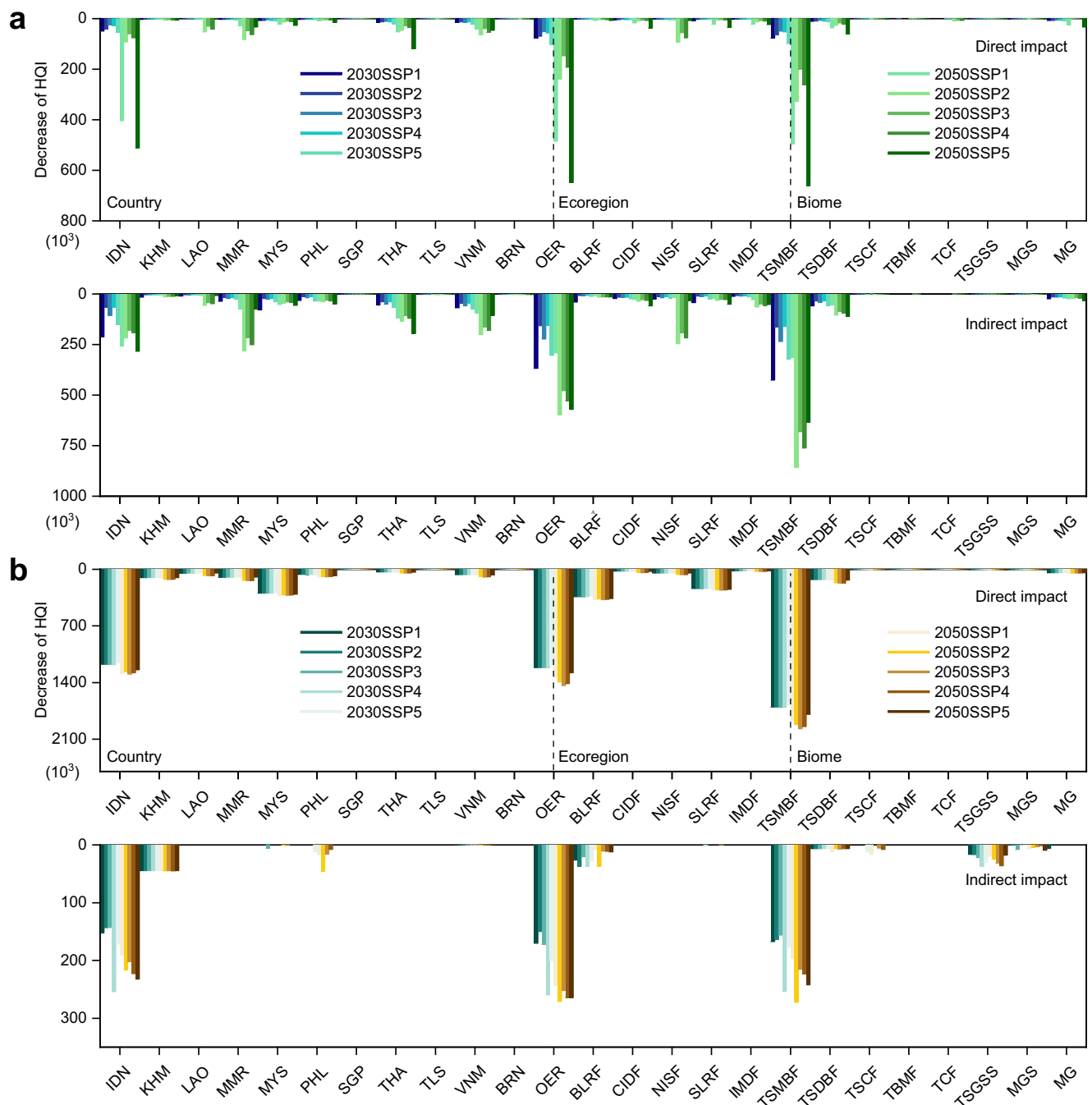


Fig. 5 | Direct and indirect impacts of urban and cropland expansions on natural habitats in 2030 and 2050 under the various SSPs. a Direct and indirect impacts of urban expansion at three scales; and **(b)** direct and indirect impacts of cropland expansion at three scales. The bars in **(a, b)** represent the decrease value of HQI.

substantial natural habitat loss and has had large impacts on natural habitats.

Among the ecoregions, the OER and lowland rainforest ecoregions (mainly BLRF and SLRF) also exhibited extensive urban and cropland expansions. The OER mainly overlaps with tropical rainforest areas, whereas the BLRF and SLRF are lowland rainforest areas. Research has shown that the formation of deforestation hotspots in Southeast Asia is driven not only by the reduction in tropical forests but also by the logging of lowland rainforests⁶. The large-scale logging of these lowland rainforests is closely linked to cropland expansion and also facilitates urban expansion to some extent.

Similarly, urban and cropland expansions also occurred in the TSMBF and TSDBF, which are representative of broadleaf forests, and

in MG biome. TSMBF, which is the main habitat for the most important tree types (tropical and subtropical broadleaf forests) in Southeast Asia, occupies 83.21% of the land area in Southeast Asia. Deforestation in tropical forests is the main reason that Southeast Asia has become a forest loss hotspot⁶. Encroachment on these lands can serve agricultural or urbanization needs, and there is considerable impetus to obtain high economic value from broadleaf forests, which possess greater tree diversity and carbon storage capacity than coniferous forests do²⁸.

Urban and cropland expansions lead to different impacts on natural habitats. The impact of cropland expansion on natural habitats is primarily direct, whereas urban expansion predominantly leads to indirect impacts. Both urban expansion and cropland expansion have

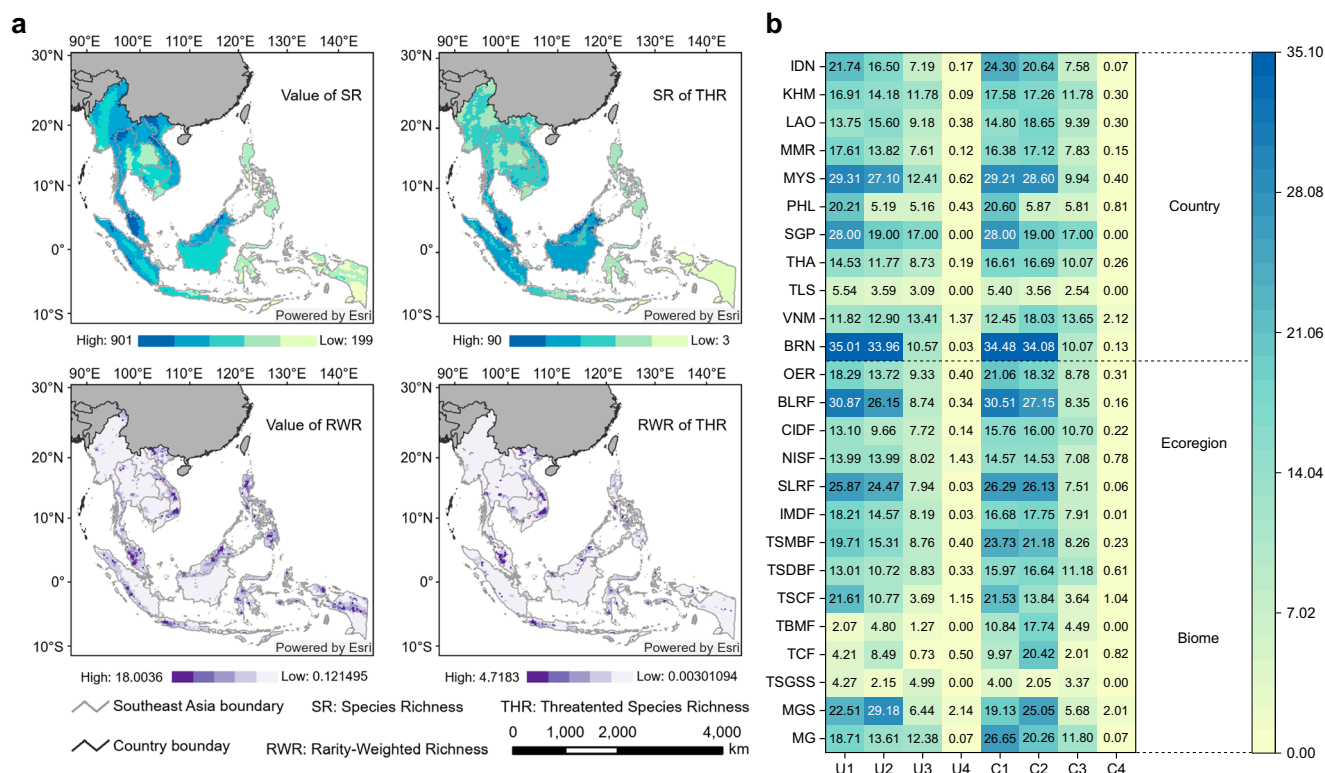


Fig. 6 | Spatial patterns of SR and RWR in Southeast Asia and THR affected by urban and cropland expansions (references to the species richness and rarity-weighted richness data are provided in the Methods and Data availability sections, and the national administrative boundaries were derived from the Global Administrative Areas: www.gadm.org). a Spatial patterns of SR and RWR and **(b)** THR number affected by urban and cropland expansions. U1 threatened

birds affected by the indirect impacts of urban expansion, U2 threatened mammals affected by the indirect impacts of urban expansion, U3 threatened reptiles affected by the indirect impacts of urban expansion; U4: threatened amphibians affected by the indirect impacts of urban expansion; similarly, C1–4 are threatened species affected by the direct impacts of cropland expansion.

been recognized as major drivers of natural habitat loss^{14,15,29,30}; however, the differences in how these two expansions affect natural habitats have not received adequate attention. The indirect impact of urban expansion can be 10 to 15 times greater than the direct impact³. Urban expansion indirectly affects natural habitats by encroaching on non-natural habitats and increasing disturbances to adjacent regions. For example, disturbances such as trampling, heavy metal pollution and urban runoff pollution, which occur within the 10 km maximum influence distance of urban land, can degrade habitat quality and disrupt regional ecological balance. In this study, we also found that the indirect impact of urban expansion in Southeast Asia from 2000 to 2020 was pronounced, being 13.76 times greater than the direct impact. However, the gap between the indirect and direct impacts will gradually decrease in 2030 and 2050 under the various SSPs, reaching approximately 1.03–5.30 times. As urbanization in Southeast Asia accelerates to reach a state of stable increase, the abundant tropical rainforest resources there will be subjected to accelerated encroachment due to urbanization, with a rapid increase in the direct impact of urban expansion.

To achieve the United Nations goal of transforming agri-food systems in the Asia-Pacific region and satisfying national agricultural security needs, there must be a reduction in the occurrence of urban encroachment into large areas of cropland, in turn limiting the rate of accumulation of indirect impacts resulting from urban expansion. We cannot deny the efforts made by governments in Southeast Asia to protect forests, such as the Reducing Emissions from Deforestation and Forest Degradation (REDD+) program, Heart of Borneo or the distinctive policies adopted by various governments for forest conservation. The differentiated national conditions and policies indicate that forest protection cannot be generalized, and some countries may

have achieved the goal of forest cover enhancement. However, we must recognize that this goal is only a target that might be achieved under the most ideal SSP1 scenario, as the SSPs official documents emphasize that the SSP1 scenario focuses on the diffusion of green growth and green economy strategies^{6,31–33}. In addition, land use is strictly regulated under SSP1, which greatly reduces the rate of deforestation in tropical forests. In this context, a series of international initiatives and declarations, such as the United Nations' Sustainable Development Goals (SDGs), the New York Declaration on Forests, and the Paris Agreement, may also play important roles in providing guidance and paths toward sustainability.

We found that because urban expansion encroaches more on non-natural habitats, its indirect impacts are more prominent, and the gap between the indirect and direct impacts has gradually decreased over time. In general, urban expansion encroaches into cropland areas with low habitat suitability⁵, and studies have indicated that by 2030, approximately 80% of cropland loss due to global urban expansion is expected to occur in Asia and Africa³⁴. We also found that between 2000 and 2050, urban expansion will still occur mainly in non-natural habitats, and cropland will be the main type of non-natural habitat occupied by urban expansion, accounting for more than 90% of the total area of urban expansion. This may result in the indirect impacts of urban expansion being more extensive than the direct impacts¹³, subsequently affecting the surrounding natural habitats with high habitat suitability.

The total impact of cropland expansion in Southeast Asia from 2000 to 2020 was 15.83 times greater than that of urban expansion, and the total impact will decrease to 1.29–6.68 times in 2030 and 2050 under the various SSPs. This may be due to cropland areas occupying approximately 40% of Southeast Asia, whereas urban areas represent

less than 1% of the total area. The global oil palm area rose from 10.40 million ha to 28.74 million ha during the 2000–2020 period³⁵, and Southeast Asia accounted for more than 86% of the global palm oil production²⁶. This surge of oil palm agriculture has resulted in deforestation. In this study, the area of cropland expansion was 1.02 to 3.47 times greater than that of urban expansion from 2000 to 2050, which is the leading driver of the high impact of cropland expansion compared to that of urban expansion. Studies have also indicated that 27.0×10^4 km² of forest in Southeast Asia has been displaced by cropland expansion¹⁰, and of this new cropland, 8.2×10^4 km² of cropland is located in highland regions of Southeast Asia¹. Highlands are ecologically sensitive and serve as critical habitats for biodiversity preservation, as well as essential water towers for lowland population centers³⁶. The occupation of highland agriculture can accelerate the fragmentation of natural habitats³⁷, which may be one of the key factors contributing to the more pronounced impacts of cropland expansion.

The direct impact of cropland expansion far exceeds the indirect impact from 2000 to 2050, indicating that cropland expansion exerts a dominant direct impact on natural habitats. Previous studies have explored the natural habitat loss caused by cropland expansion, with global cropland expansion occurring at the expense of 2 to 10 million km² of natural habitat, was projected to threaten 20,000 species by 2050^{10,29}. Cropland expansion in Southeast Asia has occurred primarily through direct encroachment into natural habitats. In this study, forests, as a component of natural habitats in Southeast Asia, were estimated to occupy approximately 40–42% of the total land area, and approximately 89–90% of the total cropland expansion area occurred via transformation from forests between 2000 and 2050. In the case of indirect impacts, the area of non-natural habitats occupied by cropland expansion was very small; therefore, we did not observe the indirect impacts of cropland expansion across all scales.

We further investigated the impacts of urban expansion and cropland expansion on threatened species. Our findings revealed that regions of high relative importance for Southeast Asian species are predominantly distributed in coastal zones (Fig. 6a). The coastal regions or islands in Southeast Asia are hotspots for mangrove forests, where natural resources are abundant. Island regions typically support a relatively large number of species that are susceptible to extinction³⁸, rendering them crucial habitats for the migration routes of many species. An example is the East Asian–Australasian Flyway (EAAF), which passes through the coastal areas of several countries in Southeast Asia. This flyway serves as a home for more than 5 million migratory waterbirds, including 36 globally threatened species, and 19 species that are considered near-threatened (<https://www.eaaflyway.net/the-flyway/>). The fact that coastal mangrove destruction suffered less than expected is a testament to the long-term, stringent management of these coastal forests in various countries, suggesting that the effective conservation of the remaining small patches of mangroves may also occur³⁹.

We found that both urban expansion and cropland expansion most prominently affected threatened bird species, followed by mammals and amphibians, which is consistent with the findings of previous studies^{38,40}. Birds and amphibians may face varying degrees of threats because birds exhibit large habitats that overlap with areas of urban and cropland expansions⁴⁰, increasing their susceptibility to impacts. In contrast, amphibians often live in complex terrains that are less likely to be occupied, where the probability of urban and cropland expansions is lower. Brunei has the highest average value of affected threatened birds and mammals across all scales. Brunei's tropical rainforests encompass more than 70% of its total land area, making Brunei one of the most forest-rich countries in the world; however oil and gas extraction has accelerated ecosystem degradation⁴¹, disrupting ecological balance and threatening species survival. The greatest impacts on threatened birds and mammals in all ecoregions were

shown in the lowland rainforest ecoregions (BLRF and SLRF), where extensive deforestation has occurred¹⁶. Only 8% of the remaining forest areas in BLRF and 7% in SLRF are protected. This leaves unprotected forests and their wildlife exceedingly susceptible to the impacts of rubber, oil palm, paper, and pulp plantations; commercial hunting; and logging.

Urban and cropland expansions have pronounced impacts on threatened species in montane and mangrove ecosystems. More than 85% of global birds, mammals, and amphibians live in montane forest ecosystems, which are sensitive to climate change and human pressures⁴². Although urban expansion has not directly spread into montane forest areas, we observed a pronounced response of threatened species caused by the indirect impacts of urban expansion in MGS. Under the direct impacts of cropland expansion, MG exhibited the greatest average value of affected threatened birds and mammals. Mangroves, which are located primarily along the coasts of Southeast Asia, face threats from cropland expansion, which can lead to local climate change, such as variations in microclimates, posing a threat to mangrove species adapted to specific climatic conditions²⁹. Additionally, compared with other biomes, MG, encompassing coastal biomes, may experience exacerbated coastal erosion. With rising sea levels caused by global climate change, the habitats of mangroves could become inundated by seawater, affecting species survival⁴³.

In this study, we found that the indirect impacts of urban expansion in Southeast Asia may surpass the direct impacts, whereas cropland expansion exhibited pronounced direct impacts. These expansion processes not only drive continuous natural habitat loss but also intensify survival pressures on threatened species (particularly birds and mammals) in this biodiversity hotspot.

To mitigate the indirect impacts of urban expansion, interventions should prioritize three dimensions: urban form, spatial planning, and transportation systems. First, the adoption of compact planning strategies with vertical greening initiatives, modeled after Singapore's high-density development paradigm⁴⁴, could optimize spatial configurations to reduce horizontal sprawl and environmental thermal pollution, thereby constraining the spatial extent of indirect impacts. Concurrently, establishing multi-center cluster layouts (e.g., Kuala Lumpur's triangular structure) with reserved ecological corridors would mitigate population pressures and block the transmission of indirect disturbances such as heavy metal pollution and runoff pollution. Furthermore, given the motorcycle-dominated private transportation in Southeast Asia⁴⁵, optimizing rail transit systems and promoting public transportation transitions can reduce road encroachment into ecological fringe areas, serving as critical measures to alleviate the indirect impacts of expansion.

Although we emphasized the importance of the indirect impacts of urban expansion, the direct impacts merit equal attention, as they can cause a complete change in the land structure. In this study, we also found that the direct impact of urban expansion caused a greater decrease in habitat quality per unit area than the indirect impact. To address direct impacts of urban expansion in Southeast Asia, strict delineation of ecological protection and urban growth boundaries is imperative, incorporating critical ecosystems such as mangrove and peat swamp forests into permanent protection to minimize direct habitat encroachment. For the degraded habitats, implementing soil remediation and native vegetation restoration programs will help rebuild ecological functions. Simultaneously, promoting regional industrial restructuring towards digital technology (e.g., e-commerce, and fintech) and ecotourism can reduce reliance on land-intensive development, fundamentally mitigating the direct impacts of occupying ecological land.

Cropland expansion has resulted in greater natural habitat loss than urban expansion in Southeast Asia (Fig. 2), primarily through direct impacts, which are closely linked with agricultural structures. Within the context of cropland expansion, market-driven forces and

the demand for economic crops have promoted the rapid agricultural development^{46–48}. To address the direct habitat encroachment into cropland areas, the following comprehensive strategies involving agricultural modernization, land rehabilitation, and technology-system integration are proposed. We recommend optimizing cultivation structures through agroforestry systems (e.g., oil palm intercropping with high-value crops) and intensive agricultural systems (e.g., rice-fish symbiosis) to minimize wetland and native ecosystem degradation. Precision drip irrigation and soil sensor technologies should be deployed to improve cropland productivity, thereby curbing aggregate land demand. Additionally, biochar application coupled with green manure rotation should be prioritized for rehabilitating degraded croplands.

Given the extensive expansion of cropland in Southeast Asia, nonpoint sources of disturbances (e.g., fertilizers and pesticides) from agriculture require urgent attention. Solutions such as the use of organic fertilizers, biological pest control training, and precision fertilization technologies can be promoted to reduce chemical inputs. Agricultural nonpoint source pollution management systems, complemented by ecological ditches and constructed wetlands, should be deployed to intercept runoff and mitigate pollution, which can contribute to indirect impacts. Additionally, the targeted recycling of agricultural waste, such as composting crop residues (e.g., rice straw, oil palm empty fruit bunches) to produce organic fertilizers, or the use of anaerobic digestion systems to convert livestock manure and rubber processing wastewater into biogas and nutrient-rich amendments, can be prioritized to further mitigate nonpoint source pollution. Enhancing the monitoring of critical habitats for birds and mammals is essential to ensure that agricultural activities do not compromise ecological integrity, to foster regional synergies between ecological conservation and sustainable agricultural development.

The dynamic trade-offs between natural habitat and land expansion are long-term challenges; thus, strengthening global cooperation has emerged as a critical imperative. To achieve the targets of SDG 15 and the Kunming–Montreal Global Biodiversity Framework, we call for a concerted effort from the governments of Southeast Asian countries, civil society, and local communities to enhance cooperation and support from the international community and promote natural habitat conservation and biodiversity preservation in Southeast Asia.

This study has certain potential uncertainties and limitations. We used the 300 m global land use dataset from the ESA to map the natural habitats in Southeast Asia from 2000 to 2020 and simulate LUC for 2030 and 2050. Some studies have used more precise land use datasets (e.g., 30 m resolution) to conduct research^{10,49}. However, this was challenging in the PLUS model simulation. The PLUS model, an improved cellular automaton, cannot handle large-scale and high-resolution simulation tasks^{50,51}. Therefore, we chose the ESA LUC dataset and successfully achieved our initial design objectives.

We chose the PLUS model because of its relatively high accuracy and advantages in simulating different scenarios compared with other models^{50,51}. However, it may also produce some uncertainties. First, the PLUS model offers a module for predicting land demand. However, we used the future demand for urban land determined by linear regression model and input it into the PLUS model. This influenced the original predicted land demand in the PLUS model, potentially resulting in some uncertainties. Second, we encountered difficulties in setting the simulation parameters. Owing to the large and extensive Southeast Asian area, running the model with default patch parameters did not achieve the spatial allocation of land use demand. We ultimately determined the patch simulation parameters by adjusting each parameter from small to large while keeping the other parameters constant. This, however, may have increased the probability of expansion in some small patch areas, potentially affecting the simulation results.

In this study, when assessing the HQI, we used the parameter framework from Ren et al.³, and assumed that the suitability and sensitivity of the same LUC type were consistent^{3,10}. Although this framework has proven effective at the global scale²⁰, these parameters may still vary across different ecoregions and agricultural types within Southeast Asia, which may have introduced some uncertainties. In addition, the indirect impacts of urban and cropland expansions were estimated using a conservative method³. We only considered the neighboring impacts within the maximum influence distances of the expansions, without considering indirect impacts such as the long-distance impacts, including the telecoupling effects of the food system and the consequences of air pollution^{3,10,52}. Moreover, our results indicated that the direct impacts of cropland expansion in Southeast Asia strongly surpassed the indirect impacts. This is because indirect impacts have a shorter influence distance, making them much smaller than direct impacts, which may lead to conservative results. For instance, the use of fertilizers and pesticides in croplands results in the wide diffusion of pollutants, especially in water, the long-term indirect impacts of cropland expansion may be underestimated. Additionally, we employed a spatial overlay approach to assess the impacts of urban and cropland expansions on threatened species. While this relatively straightforward method has been prevalently applied in related studies, it may have some limitations, as only the number of affected threatened species is estimated without revealing the specific degree of their impacts^{40,53,54}.

Methods

Land use and cover map

The global LUC data with a 300 m spatial resolution during 2000–2020 were obtained from the European Space Agency (ESA) Climate Change Initiative Land Cover dataset, which is one of the most accurate land use datasets available^{3,55}. This dataset covers multiple temporal points and captures long-term LUC changes, with an overall accuracy of 71%^{3,56}. To assess natural habitat loss and spatiotemporal dynamics of urban and cropland expansions in Southeast Asia, we obtained LUC data for 2000, 2010 and 2020. These data were categorized into eight classes^{57,58}: cropland, forestland, grassland, wetland, urban, shrubland, bare land, and water. Furthermore, in accordance with the International Union for Conservation of Nature (IUCN) criteria^{3,59}, natural habitats were defined as forestland, grassland, wetland, shrubland, and water. We then used LUC data to determine the spatial distribution of natural habitats across Southeast Asia at three scales (country, ecoregion and biome). We calculated the expansion area and the corresponding rate of change based on urban and cropland data, and generated dynamic maps of urban and cropland expansions from 2000 to 2020 (Fig. 2 and Supplementary Figs. 3–5). LUC data from 2000, 2010, and 2020 were subsequently employed to simulate LUC patterns in 2030 and 2050 under the various SSPs.

Boundaries of the ecoregion and biome

We mapped the spatial distribution of natural habitat loss across various ecoregions and biomes. We utilized the World Wildlife Fund's (WWF) terrestrial ecoregions dataset (<https://www.worldwildlife.org/publications/terrestrial-ecoregions-of-the-world>), which is a biogeographic classification of the terrestrial ecosystems, with the world divided into 867 ecoregions and 14 biomes. In this study, we extracted boundaries for 86 ecoregions and 8 biomes in Southeast Asia. To analyze the natural habitat loss of the most representative ecoregions in Southeast Asia and provide a reference for the scale analytical framework, referring to previous studies^{3,60,61}, we selected the five largest ecoregions by area, which span a variety of climatic and topographical conditions, from lowlands to mountains and from dry to moist environments; this approach captured the unique ecological characteristics

of Southeast Asia, and merged the remaining ecoregions (labelled as other ecoregions, OER). Finally, six ecoregions were obtained. We then assessed the natural habitat loss and the dynamics of urban and cropland expansions in Southeast Asia from 2000 to 2050 at three scales (i.e., country, ecoregion, and biome) (Supplementary Figs. 1 and 2).

Descriptions of future scenarios

To evaluate the future impacts of urban and cropland expansions on natural habitats in 2030 and 2050, we employed the Shared Socioeconomic Pathways (SSPs)^{31–33,62,63}. These pathways encompass development characteristics such as socioeconomic growth, technological advancement, and climate change adaptation strategies. The SSPs comprise a set of global narrative scenarios based on socioeconomic assumptions, encompassing five distinct development models associated with future socioeconomic scenarios^{31–33,62,63}. Specifically, SSP1 (sustainability—taking the green road) represents a sustainable development scenario, emphasizing a shift from accelerated economic expansion to prioritizing human well-being in the future. SSP2 (middle of the road) represents an intermediate development scenario in which most economies are politically stable and follow historical development patterns. SSP3 (regional rivalry—rocky road) represents a regional competition scenario with slow economic growth and urbanization. SSP4 (inequality—road divided) represents an uneven development scenario characterized by rapid urbanization growth in relatively lower-income regions and a decrease in relatively higher-income regions. SSP5 (fossil-fueled development—taking the highway) represents a rapid global economic development scenario and a high-growth model at the expense of substantial fossil fuel use.

Forecasting the future urban demand

To obtain the future urban areas for the various SSPs, we extracted the urban land from the ESA LUC data during 2000–2020 and obtained the Gross Domestic Product (GDP) data for Southeast Asia from the World Bank (<https://data.worldbank.org/indicator/NY.GDP.MKTP.CD>). A linear regression model was employed to determine future urban land areas under different pathways^{2,40,64}. In this study, the linear regression model was chosen due to its excellent interpretability and ability to identify relationships among variables². The use of linear regression models to predict future urban expansion under SSP scenarios has been applied at the global scale^{2,40}. We assume that with increasing GDP, the urban land area will expand^{2,40}. The historical GDP data for Southeast Asia as the independent variable and the historical urban land area as the dependent variable, we established the following linear regression equation:

$$U_i = 0.604 \times \text{GDP}_i (\text{hundred million}) + 16096.326 \quad (1)$$

where U_i denotes the urban demand in the i^{th} year and GDP_i denotes the GDP of Southeast Asia in the i^{th} year. The coefficient of determination (R^2) for the linear regression model was 0.93, indicating that the model accounts for 93% of the total variation in the dependent variable. After the t test, the P -values were found to be less than 0.05, demonstrating that the model results were statistically significant and met the test criteria.

We extracted data from the Gridded Datasets for Population and Economy under the Shared Socioeconomic Pathways (<https://doi.org/10.57760/sciencedb.01683>) to obtain the corresponding GDP data for Southeast Asia in 2030 and 2050. Since these data have a 0.5° spatial resolution, to ensure the spatial consistency, we further resampled them to a 300 m resolution. Then, we extracted the GDP data for the SSPs and substituted the obtained GDP data into Eq. (1), to determine the demand for urban land in the five SSPs.

Land use and cover simulation

Utilizing the the Patch-generating Land Use Simulation (PLUS) model, we projected the spatial distribution of land use in 2030 and 2050 on the basis of the predicted urban land areas and the LUC data during 2000–2020. The PLUS model, which is recognized for yielding higher simulation accuracy compared with models such as FLUS and LUSD^{50,51}, incorporates a Land Expansion Analysis Strategy (LEAS) that operates within a rule-mining framework, along with a Cellular Automaton module that employs the Multi-type Random Patch Seeds (CARS) approach⁵⁰. This integrated approach allows the model to simulate changes in LUC patches and better represent complex LUC systems.

In this study, we used three major modules of the PLUS model to verify accuracy and simulate future LUC: the extraction of land expansion, LEAS, and CARS modules. The extraction of land expansion module is used to determine the expansion of various land uses by analyzing LUC data from two periods. By comparing the LUC data from 2000 to 2010, we identified areas of change that represented the transformation of land use types (e.g., the conversion of cropland to urban land). We then input the LUC data into the module, yielding a land expansion map. The LEAS module is subsequently run to obtain the development potential and transformation rules for various land uses from the land expansion map via a random forest algorithm. This process requires the input of socioeconomic and climatic factors to help capture the expansion patterns of land use types. Additionally, we selected 12 relevant driving factors (Supplementary Table 14) and unified their spatial resolution to 300 m before inputting them into the PLUS model. Thus, we obtained development potential maps for various LUC types, which are closely associated with the spatial allocation of subsequent land use simulations.

After the patterns and potential of land expansion were determined, the CARS module, with random seed generation and a threshold attenuation mechanism integrated, was employed to spatially and temporally simulate the autonomous formation of land patches dynamically under the constraints of development potential. First, the PLUS model provides a module for predicting the land demand. We input the LUC data from 2000 and 2010 to obtain the demand for eight land use types in 2020. In the simulations for 2030 and 2050, we replaced the demand for urban land generated by the module with the future demand for urban land obtained from the linear regression model. After confirming the land demand, we set the patch parameters to effectively allocate these land demands for various land patches. These patch parameters, together with the previously determined development potential of the land, were used to jointly determine the final total probability of land use conversion. An increased total probability enhances the chance that a particular land type will be prioritized for allocation. Among these patch parameters, the patch generation threshold acts as an attenuation threshold for creating new patches, with values between 0 and 1, and a default setting of 0.5. A high threshold indicates a more conservative approach to conversion. The expansion coefficient, another parameter that influences the model's potential to create new land use patches, also ranges from 0 to 1, with a default setting of 0.1. A large expansion coefficient denotes a high probability of generating new patches. In addition, the parameter for seed percentage serves as the maximum threshold for determining the quantity of new seeds generated, within a range of 0 to 1, typically initialized at 0.0001. A high seed percentage results in a widespread distribution of land use patterns.

In this study, owing to the vast area of Southeast Asia and the complex structure of land use patches, the default parameters could not be used to perfectly allocate the spatial pattern of LUC. Therefore, we discarded the default values of these three parameters and adjusted each parameter from small to large while keeping the other parameters constant. Ultimately, we selected the combination of

parameters that best achieved the simulation objectives and yielded the highest simulation accuracy. The patch generation threshold was set to 0.2, the expansion coefficient was 0.9, and the seed percentage was 0.1.

Subsequently, we simulated LUC dynamics in 2020; the kappa coefficient obtained was 0.912, whereas the overall accuracy of the model was 0.949, indicating a high level of precision⁶⁵. This suggests that the LUC simulations are reliable predictions. We then simulated LUC dynamics in 2030 and 2050 under the five SSPs based on the LUC data for 2020 and used the expansion area and expansion rate to create graphs of urban and cropland expansions (2000–2030 and 2000–2050) (Fig. 4).

Urban and cropland expansions dynamics

We employed the expansion area and expansion rate indicators to evaluate the dynamic processes of urban expansion and cropland expansion^{66,67}, and further assessed the dynamics of urban expansion and cropland expansion in Southeast Asia, as well as the expansion area and expansion rate at three scales (Fig. 2, Supplementary Figs. 3–5), with the following equations:

$$EA_{(n,m)} = A_m - A_n \quad (2)$$

$$ER_{(n,m)} = \left(\left(\frac{A_m}{A_n} \right)^{\frac{1}{m-n}} - 1 \right) \times 100\% \quad (3)$$

where $EA_{(n,m)}$ represents the changes in the urban or cropland areas from the n^{th} to the m^{th} year. The areas of urban or cropland in the n^{th} and m^{th} years are represented by A_n and A_m , respectively, and $ER_{(n,m)}$ denotes the urban expansion rate or cropland expansion rate from the n^{th} to the m^{th} year.

Habitat quality evaluation

The HQI is used to evaluate the level of habitats needed to support the survival and development of species based on their suitability and the intensity of habitat degradation^{3,10}. The HQI is derived primarily from self-defined biodiversity values for broad land cover types, with a penalty for proximity to urban areas and croplands. As a dimensionless value ranging from 0 to 1, high values typically reflect the ability to support biodiversity at all levels within a given area^{21,22}. In this study, we adopted the HQI parameter framework developed by Ren et al.³, and generated the index using the InVEST model^{21,22}. These parameters are determined using expert knowledge scoring method and exploratory ensemble modeling approach³, and have been used to assess the HQI at the global scale²⁰. Specifically, we utilized the HQI to assess the direct and indirect impacts of urban and cropland expansions during 2000–2020 (Fig. 3), and combined it with the PLUS model to further assess the impacts in 2030 and 2050 (Fig. 5). The specific equations of the HQI are as follows:

$$HQI_{xj} = H_j \left(1 - \left(\frac{D_{xj}^z}{D_{xj}^z + k^z} \right) \right) \quad (4)$$

$$D_{xj} = \sum_{r=1}^R \sum_{y=1}^{Y_r} \left(\frac{w_r}{\sum_{r=1}^R w_r} \right) r_y i_{rxy} \beta_x S_{jr} \quad (5)$$

$$i_{rxy} = 1 - \left(\frac{d_{xy}}{d_{rmax}} \right) \text{ if linear} \quad (6)$$

$$i_{rxy} = \exp \left(- \left(\frac{2.99}{d_{rmax}} \right) d_{xy} \right) \text{ if exponential} \quad (7)$$

We employed a semi-saturation function to convert the degradation score for a given pixel into a HQI value. According to the InVEST guidelines²¹, the semi-saturation value k is typically set to half the maximum degree of degradation, that is, 0.5. This value only determines the distribution and central tendency of the HQI score^{3,21}, with z serving as a constant, usually set to 2.5^{21,22}. With increasing degradation score of a pixel, its HQI decreases. The HQI of pixel x within LUC class j is denoted by HQI_{xj} , and it ranges from 0 to 1. When the value is close to 1, this indicates a robust ecosystem capable of providing optimal conditions for the sustenance of species and individuals. H_j signifies the habitat suitability for LUC class j ; a high value suggests high potential for the habitat to support species survival. The habitat threat level of pixel x within LUC class j is denoted as D_{xj} . Moreover, R represents the aggregate count of threat sources, which are generally considered anthropogenically transformed LUC types that can lead to habitat fragmentation, edge effects, and degradation in adjacent habitats^{3,21,22}.

Referring to Ren et al.³, we defined urban, cropland, and road as threat sources (Supplementary Table 12). The threat source weight w_r is used to quantify the relative influence of threat source r on habitats, and r_y represents the threat source r within pixel y . Furthermore, i_{rxy} indicates the impact of threat source r on the habitat pixel x in pixel y , with β_x occurring within the range of [0, 1], representing the accessibility of various threat sources in pixel x . Finally, the sensitivity of LUC type j to threat r is given by S_{jr} (Supplementary Table 13); d_{xy} is the spatial distance between pixels x and y , which varies according to the spatial decay type of each threat, whether linear or exponential; and d_{rmax} is the maximum influence distance for threat source r . Subsequently, we assessed the HQI and its pattern under each SSP scenario in 2030 and 2050 and derived direct and indirect impacts.

Habitat quality validation

Since the HQI is generated through LUC and threats to biodiversity, the HQI has been evaluated with species richness data, and a positive relationship has been obtained between the number of species and the HQI^{3,22}; however, a low HQI does not necessarily indicate a low biodiversity conservation value in an area³. Furthermore, in this study, the HQI is calculated based on LUC data, and scholars have similarly employed the normalized difference vegetation index (NDVI) and net primary productivity (NPP), which reflect the net increase and growth status of vegetation^{68,69}, to study their relationships with the HQI^{3,60,70,71}. Some researchers have used correlation analysis to reveal a positive relationship between the HQI and NDVI, suggesting that the NDVI can, to some extent, be used to verify the quality of regional natural habitats^{70,72}.

In this study, we used the NDVI and NPP to validate the effectiveness of the HQI at the ecoregion scale. Ecoregions typically have relatively consistent environmental characteristics and vegetation types⁷³. Therefore, to capture the overall relationship between the HQI and NDVI, NPP, we performed a correlation analysis using the mean HQI, NPP, and NDVI values in 2010 across the 86 ecoregions to verify the effectiveness of the HQI. The NPP and NDVI were obtained from the MOD17A3 dataset and PKU GIMMS NDVI dataset, and the annual mean maps of the NPP and NDVI were synthesized and resampled them to 300 m. Then, the units of NPP were scaled ($\text{g C m}^{-2} \text{ year}^{-1}$) and we obtained the average NDVI and NPP of each ecoregion. The results indicated a positive relationship between the HQI and both the NPP and the NDVI (Supplementary Fig. 7).

Assessing the impacts of urban and cropland expansions on natural habitats

We used a proportion indicator to represent the total impact (the sum of direct and indirect impacts), that is, the proportion of the HQI decrease due to urban and cropland expansions relative to the total HQI decrease. The direct impact is defined as the decrease in the HQI

caused by the direct encroachment of urban and cropland areas into natural habitats. The indirect impact is defined as the decrease in the HQI associated with urban and cropland expansions into non-natural habitats within the maximum influence distances of urban and cropland areas (Supplementary Fig. 6). Here, we followed the parameters used by Ren et al.³, the maximum influence distances for urban and cropland were established at 10 km and 2 km, respectively. When calculating these two types of impacts, we assumed that only urban land underwent changes during urban expansion and that only cropland exhibited changes during cropland expansion, ensuring that there was no interference from other land use changes³. Moreover, we focused exclusively on displacement due to urban and cropland expansions, without accounting for the regenerative capacity of natural habitats.

$$TI_{HQI} = DI_{HQI} + IDI_{HQI} \quad (8)$$

$$DI_{HQI} = \sum_{i=1}^n (HQI_d \times i_e) \quad (9)$$

$$IDI_{HQI} = \sum_{j=1}^m (HQI_d \times j_e)_{mid} \quad (10)$$

where TI_{HQI} denotes the total impact caused by urban expansion or cropland expansion. The DI_{HQI} and IDI_{HQI} represent the HQI reduction resulting from the direct impact and indirect impact of urban expansion or cropland expansion, respectively. With the period of 2000–2020 as an example, HQI_d is the difference in habitat quality on the basis of the difference between the HQI value in 2020 and that in 2000, where a negative HQI_d indicates a decrease in habitat quality.

The direct impact is the decrease in the HQI caused by the direct encroachment of urban or cropland into natural habitats, n represents the number of natural habitat pixels and i_e is a Boolean variable in Eq. (9). A value of 1 indicates that the i^{th} natural habitat pixel has been encroached upon by urban expansion or cropland expansion, whereas a value of 0 means that the pixel has not been encroached upon. Similarly, the indirect impact is the decrease in the HQI caused by non-natural habitats occupied by urban expansion or cropland expansion within a maximum influence distance. Therefore, in Eq. (10), m represents the number of non-natural habitat pixels. When j_e equals 1, urban expansion or cropland expansion has encroached upon the j^{th} non-natural habitat pixel; when j_e equals 0, the pixel has not been encroached upon. mid refers to urban expansion within a maximum influence distance of 10 km or cropland expansion within a maximum influence distance of 2 km.

Assessing the impacts of urban and cropland expansions on threatened species

To quantify the potential impacts of natural habitat loss due to urban and cropland expansions on species diversity, we obtained species richness (SR) and rarity-weighted richness (RWR) data for four types of terrestrial vertebrates from the IUCN: mammals, birds, amphibians, and reptiles, which represents the species diversity of Southeast Asia. This dataset also includes the SR and RWR of threatened species, which are distributed spatially at a 10 km resolution. SR signifies the possible number of species potentially found in each pixel, whereas RWR represents the aggregate importance of each pixel to the species occurring within it. The value of RWR is non-dimensional, indicating relative importance. We acquired SR and RWR data for all species and threatened species (critically endangered, endangered, and vulnerable) in Southeast Asia (Fig. 6a), and resampled them to a 300 m resolution to align with other data. Then, we used a spatial overlay approach to assess the impacts of urban and cropland expansions on

threatened species^{2,40,53}. In this study, if the natural habitat loss caused by urban and cropland expansions overlapped with the distribution of threatened species, we determined that the species to be affected by urban and cropland expansions and included it in the set of affected species. Specifically, we overlapped the SR and RWR data with the extent of natural habitat loss attributed to urban and cropland expansions to obtain the affected number of threatened species at three scales (Fig. 6b).

Data availability

The LUC data were sourced from the European Space Agency (ESA) Climate Change Initiative Land Cover (ESA CCI LC) dataset: <https://www.esa-landcover-cci.org/>. The PLUS model were obtained from https://github.com/HPSCIL/Patch-generating_Land_Use_Simulation_Model. The road data were extracted from the Global Roads Open Access Data Set, version 1 (gROADSV1), which can be downloaded from <https://sedac.ciesin.columbia.edu/data/set/groads-global-roads-open-access-v1>. The national administrative boundaries for Southeast Asian countries were obtained from the Global Administrative Areas: www.gadm.org. The boundaries of the ecoregions and biomes were obtained from the World Wildlife Fund's terrestrial ecoregions: <https://www.worldwildlife.org/publications/terrestrial-ecoregions-of-the-world>. The NPP was obtained from <https://lpdaac.usgs.gov/products/mod17a3hgf061/>. The NDVI values were derived from the PKU GIMMS NDVI, version 1.2 dataset: <https://doi.org/10.5281/zenodo.8253971>. Species richness and rarity-weighted richness data were derived from the International Union for Conservation of Nature (IUCN) Red List of Threatened Species: <https://www.iucnredlist.org/resources/other-spatial-downloads>. The Gross Domestic Product (GDP) data across various SSPs were sourced from <https://doi.org/10.57760/sciencedb.01683>. Geospatial data processing and corresponding figures were created using ArcGIS Pro software version 3.3.2 (<https://www.esri.com/>). All the data generated or analyzed in this study are provided in the main text and the Supplementary Information file.

References

- Zeng, Z. et al. Highland cropland expansion and forest loss in Southeast Asia in the twenty-first century. *Nat. Geosci.* **11**, 556–562 (2018).
- Li, G. et al. Global impacts of future urban expansion on terrestrial vertebrate diversity. *Nat. Commun.* **13**, 1628 (2022).
- Ren, Q. et al. Impacts of urban expansion on natural habitats in global drylands. *Nat. Sustain.* **5**, 869–878 (2022).
- Sarira, T. V., Zeng, Y., Neugarten, R., Chaplin-Kramer, R. & Koh, L. P. Co-benefits of forest carbon projects in Southeast Asia. *Nat. Sustain.* **5**, 393–396 (2022).
- Van Vliet, J. Direct and indirect loss of natural area from urban expansion. *Nat. Sustain.* **2**, 755–763 (2019).
- Estoque, R. C. et al. The future of Southeast Asia's forests. *Nat. Commun.* **10**, 1829 (2019).
- Sodhi, N. S. et al. The state and conservation of Southeast Asian biodiversity. *Biodivers. Conserv.* **19**, 317–328 (2010).
- Stibig, H.-J., Achard, F., Carboni, S., Raši, R. & Miettinen, J. Change in tropical forest cover of Southeast Asia from 1990 to 2010. *Bio-geosciences* **11**, 247–258 (2014).
- Wilcove, D. S., Giam, X., Edwards, D. P., Fisher, B. & Koh, L. P. Navjot's nightmare revisited: Logging, agriculture, and biodiversity in Southeast Asia. *Trends Ecol. Evol.* **28**, 531–540 (2013).
- Ma, S., Wang, L.-J., Jiang, J. & Zhao, Y.-G. Direct and indirect effects of agricultural expansion and landscape fragmentation processes on natural habitats. *Agric. Ecosyst. Environ.* **353**, 108555 (2023).
- Güneralp, B., Reba, M., Hales, B. U., Wentz, E. A. & Seto, K. C. Trends in urban land expansion, density, and land transitions from 1970 to 2010: A global synthesis. *Environ. Res. Lett.* **15**, 044015 (2020).

12. Guerrero-Pineda, C. et al. An investment strategy to address biodiversity loss from agricultural expansion. *Nat. Sustain.* **5**, 610–618 (2022).
13. McDonald, R. I. et al. Urban effects, distance, and protected areas in an urbanizing world. *Landsc. Urban Plan.* **93**, 63–75 (2009).
14. Liu, X. et al. High-spatiotemporal-resolution mapping of global urban change from 1985 to 2015. *Nat. Sustain.* **3**, 564–570 (2020).
15. Potapov, P. et al. Global maps of cropland extent and change show accelerated cropland expansion in the twenty-first century. *Nat. Food* **3**, 19–28 (2021).
16. Savini, T., Namkhan, M. & Sukumal, N. Conservation status of Southeast Asian natural habitat estimated using Galliformes spatio-temporal range decline. *Glob. Ecol. Conserv.* **29**, e01723 (2021).
17. Namkhan, M., Sukumal, N. & Savini, T. Impact of climate change on Southeast Asian natural habitats, with focus on protected areas. *Glob. Ecol. Conserv.* **39**, e02293 (2022).
18. Coleman, J. L. et al. Top 100 research questions for biodiversity conservation in Southeast Asia. *Biol. Conserv.* **234**, 211–220 (2019).
19. Sodhi, N. S. et al. Conserving Southeast Asian forest biodiversity in human-modified landscapes. *Biol. Conserv.* **143**, 2375–2384 (2010).
20. Yang, L., Xu, H., Pan, S., Chen, W. & Zeng, J. Identifying the impact of global human activities expansion on natural habitats. *J. Clean. Prod.* **434**, 140247 (2024).
21. Sharp, R. et al. InVEST 3.2.0 user's guide. *Nat. Cap. Proj.* **133**, <http://releases.naturalcapitalproject.org/invest-userguide/latest/> (2015).
22. Terrado, M. et al. Model development for the assessment of terrestrial and aquatic habitat quality in conservation planning. *Sci. Total Environ.* **540**, 63–70 (2016).
23. Mulligan, G. F. Revisiting the urbanization curve. *Cities* **32**, 113–122 (2013).
24. Arfanuzzaman, M. D. & Dahiya, B. Sustainable urbanization in Southeast Asia and beyond: Challenges of population growth, land use change, and environmental health. *Growth and Change* **50**, 725–744 (2019).
25. Burra, D. D. et al. Drivers of land use complexity along an agricultural transition gradient in Southeast Asia. *Ecol. Indic.* **124**, 107402 (2021).
26. Jayatilake, H. M., Jamaludin, J., De Alban, J. D. T., Webb, E. L. & Carrasco, L. R. The conversion of rubber to oil palm and other landcover types in Southeast Asia. *Appl. Geogr.* **150**, 102838 (2023).
27. Xu, Y. et al. Annual oil palm plantation maps in Malaysia and Indonesia from 2001 to 2016. *Earth Syst. Sci. Data* **12**, 847–867 (2020).
28. Li, S., Liu, W., Lang, X., Huang, X. & Su, J. Species richness, not abundance, drives ecosystem multifunctionality in a subtropical coniferous forest. *Ecol. Indic.* **120**, 106911 (2021).
29. Williams, D. R. et al. Proactive conservation to prevent habitat losses to agricultural expansion. *Nat. Sustain.* **4**, 314–322 (2020).
30. McDonald, R. I. et al. Research gaps in knowledge of the impact of urban growth on biodiversity. *Nat. Sustain.* **3**, 16–24 (2019).
31. O'Neill, B. C. et al. The roads ahead: Narratives for shared socio-economic pathways describing world futures in the 21st century. *Glob. Environ. Change* **42**, 169–180 (2017).
32. Riahi, K. et al. The shared socioeconomic pathways and their energy, land use, and greenhouse gas emissions implications: An overview. *Glob. Environ. Change* **42**, 153–168 (2017).
33. Popp, A. et al. Land-use futures in the shared socio-economic pathways. *Glob. Environ. Change* **42**, 331–345 (2017).
34. Bren d'Amour, C. et al. Future urban land expansion and implications for global croplands. *Proc. Natl Acad. Sci.* **114**, 8939–8944 (2017).
35. Yu, H. et al. Regimes of global and national oil palm cultivations from 2001 to 2018. *Glob. Environ. Change* **86**, 102845 (2024).
36. Cuo, L., Giambelluca, T. W., Ziegler, A. D. & Nullet, M. A. The roles of roads and agricultural land use in altering hydrological processes in Nam Mae Rim watershed, northern Thailand. *Hydrol. Process.* **22**, 4339–4354 (2008).
37. Yang, C. et al. Human expansion into Asian highlands in the 21st century and its effects. *Nat. Commun.* **13**, 4955 (2022).
38. Howard, C., Flather, C. H. & Stephens, P. A. A global assessment of the drivers of threatened terrestrial species richness. *Nat. Commun.* **11**, 993 (2020).
39. Richards, D. R. & Friess, D. A. Rates and drivers of mangrove deforestation in Southeast Asia, 2000–2012. *Proc. Natl Acad. Sci.* **113**, 344–349 (2016).
40. Ren, Q. et al. Impacts of global urban expansion on natural habitats undermine the 2050 vision for biodiversity. *Resour. Conserv. Recycl.* **190**, 106834 (2023).
41. Xuan, V. N. Determinants of carbon dioxide emissions in technology revolution 6.0: new insights from Brunei. *Energy Strategy Rev.* **57**, 101633 (2025).
42. He, X. et al. Accelerating global mountain forest loss threatens biodiversity hotspots. *One Earth* **6**, 303–315 (2023).
43. Wang, Y.-S. & Gu, J.-D. Ecological responses, adaptation and mechanisms of mangrove wetland ecosystem to global climate change and anthropogenic activities. *Int. Biodeterior. Biodegrad.* **162**, 105248 (2021).
44. Aydin, E. E. et al. Climate-responsive urban planning through generative models: Sensitivity analysis of urban planning and design parameters for urban heat island in Singapore's residential settlements. *Sustain. Cities Soc.* **114**, 105779 (2024).
45. Nguyen, S.-T., Moeinaddini, M., Saadi, I. & Cools, M. Unveiling the drivers of modal switch from motorcycles to public transport in Southeast Asia. *Transp. Res. Part F. Traffic Psychol. Behav.* **102**, 373–391 (2024).
46. Bruun, T. B., De Neergaard, A., Lawrence, D. & Ziegler, A. D. Environmental Consequences of the Demise in Swidden Cultivation in Southeast Asia: Carbon Storage and Soil Quality. *Hum. Ecol.* **37**, 375–388 (2009).
47. Crist, E., Mora, C. & Engelman, R. The interaction of human population, food production, and biodiversity protection. *Science* **356**, 260–264 (2017).
48. Li, F., Wu, S., Liu, H. & Yan, D. Biodiversity loss through cropland displacement for urban expansion in China. *Sci. Total Environ.* **907**, 167988 (2024).
49. Zhang, X. et al. GLC_FCS30D: the first global 30 m land-cover dynamics monitoring product with a fine classification system for the period from 1985 to 2022 generated using dense-time-series Landsat imagery and the continuous change-detection method. *Earth Syst. Sci. Data* **16**, 1353–1381 (2024).
50. Liang, X. et al. Understanding the drivers of sustainable land expansion using a patch-generating land use simulation (PLUS) model: A case study in Wuhan, China. *Comput. Environ. Urban Syst.* **85**, 101569 (2021).
51. Zhang, T., Cheng, C. & Wu, X. Mapping the spatial heterogeneity of global land use and land cover from 2020 to 2100 at a 1 km resolution. *Sci. Data* **10**, 748 (2023).
52. Yang, Y., Nan, Y., Liu, Z., Zhang, D. & Sun, Y. Direct and indirect losses of natural habitat caused by future urban expansion in the transnational area of Changbai Mountain. *Sustain. Cities Soc.* **63**, 102487 (2020).
53. Seto, K. C., Güneralp, B. & Hutyrá, L. R. Global forecasts of urban expansion to 2030 and direct impacts on biodiversity and carbon pools. *Proc. Natl Acad. Sci.* **109**, 16083–16088 (2012).
54. Powers, R. P. & Jetz, W. Global habitat loss and extinction risk of terrestrial vertebrates under future land-use-change scenarios. *Nat. Clim. Change* **9**, 323–329 (2019).
55. Gong, P. et al. Annual maps of global artificial impervious area (GAIA) between 1985 and 2018. *Remote Sens. Environ.* **236**, 111510 (2020).

56. CCI, E. L. C. Product User Guide Version 2.0. UCL-Geomat. Lond. UK **685**, http://maps.elie.ucl.ac.be/CCI/viewer/download/ESACCI-LC-Ph2-PUGv2_2.0.pdf (2017).
57. Reinhart, V. et al. Comparison of ESA climate change initiative land cover to CORINE land cover over Eastern Europe and the Baltic States from a regional climate modeling perspective. *Int. J. Appl. Earth Obs. Geoinf.* **94**, 102221 (2021).
58. Vilar, L., Garrido, J., Echavarría, P., Martínez-Vega, J. & Martín, M. P. Comparative analysis of CORINE and climate change initiative land cover maps in Europe: Implications for wildfire occurrence estimation at regional and local scales. *Int. J. Appl. Earth Obs. Geoinf.* **78**, 102–117 (2019).
59. Salafsky, N. et al. A Standard Lexicon for Biodiversity Conservation: Unified Classifications of Threats and Actions. *Conserv. Biol.* **22**, 897–911 (2008).
60. Li, X. et al. Response of vegetation phenology to urbanization in the conterminous United States. *Glob. Change Biol.* **23**, 2818–2830 (2017).
61. McDonald, R. I., Güneralp, B., Huang, C.-W., Seto, K. C. & You, M. Conservation priorities to protect vertebrate endemics from global urban expansion. *Biol. Conserv.* **224**, 290–299 (2018).
62. O'Neill, B. C. et al. A new scenario framework for climate change research: the concept of shared socioeconomic pathways. *Clim. Change* **122**, 387–400 (2014).
63. Nilsson, A. E. et al. Towards extended shared socioeconomic pathways: A combined participatory bottom-up and top-down methodology with results from the Barents region. *Glob. Environ. Change* **45**, 124–132 (2017).
64. He, C. et al. Future global urban water scarcity and potential solutions. *Nat. Commun.* **12**, 4667 (2021).
65. Mondini, A. C., Guzzetti, F. & Melillo, M. Deep learning forecast of rainfall-induced shallow landslides. *Nat. Commun.* **14**, 2466 (2023).
66. Huang, Q. et al. The occupation of cropland by global urban expansion from 1992 to 2016 and its implications. *Environ. Res. Lett.* **15**, 084037 (2020).
67. Qi, T., Ren, Q., Zhang, D., Lu, W. & He, C. Impacts of urban expansion on vegetation in drylands: A multiscale analysis based on the vegetation disturbance index. *Ecol. Indic.* **147**, 109984 (2023).
68. Chen, J., Shao, Z., Huang, X. & Hu, B. Multi-source data-driven estimation of urban net primary productivity: A case study of Wuhan. *Int. J. Appl. Earth Obs. Geoinf.* **127**, 103638 (2024).
69. Li, M. et al. Spatiotemporally consistent global dataset of the GIMMS normalized difference vegetation index (PKU GIMMS NDVI) from 1982 to 2022. *Earth Syst. Sci. Data* **15**, 4181–4203 (2023).
70. Yang, L. et al. Spatially non-stationary response of habitat quality to land use activities in World's protected areas over 20 years. *J. Clean. Prod.* **419**, 138245 (2023).
71. Zhang, X., Wan, W., Fan, H., Dong, X. & Lv, T. Temporal and spatial responses of landscape patterns to habitat quality changes in the Poyang Lake region, China. *J. Nat. Conserv.* **77**, 126546 (2024).
72. Weber, D., Schaepman-Strub, G. & Ecker, K. Predicting habitat quality of protected dry grasslands using Landsat NDVI phenology. *Ecol. Indic.* **91**, 447–460 (2018).
73. Olson, D. M. et al. Terrestrial Ecoregions of the World: A New Map of Life on Earth. *BioScience* **51**, 933 (2001).

Acknowledgements

This study was funded by Social Science Foundation of Jiangxi Province (No. 24GL39), and the Science and Technology Research Project of Jiangxi Provincial Department of Education (No. GJJ2400412).

Author contributions

X.Z.: Conceptualization, Investigation, Methodology, Formal analysis, Writing –original draft. W.W.: Methodology, Formal analysis, Visualization, Writing–original draft. R. C. E.: Investigation, Methodology, Writing–review & editing.

Competing interests

The authors declare no competing interests.

Additional information

Supplementary information The online version contains supplementary material available at <https://doi.org/10.1038/s41467-025-63384-4>.

Correspondence and requests for materials should be addressed to Xinmin Zhang.

Peer review information *Nature Communications* thanks the anonymous reviewer(s) for their contribution to the peer review of this work. A peer review file is available.

Reprints and permissions information is available at <http://www.nature.com/reprints>

Publisher's note Springer Nature remains neutral with regard to jurisdictional claims in published maps and institutional affiliations.

Open Access This article is licensed under a Creative Commons Attribution-NonCommercial-NoDerivatives 4.0 International License, which permits any non-commercial use, sharing, distribution and reproduction in any medium or format, as long as you give appropriate credit to the original author(s) and the source, provide a link to the Creative Commons licence, and indicate if you modified the licensed material. You do not have permission under this licence to share adapted material derived from this article or parts of it. The images or other third party material in this article are included in the article's Creative Commons licence, unless indicated otherwise in a credit line to the material. If material is not included in the article's Creative Commons licence and your intended use is not permitted by statutory regulation or exceeds the permitted use, you will need to obtain permission directly from the copyright holder. To view a copy of this licence, visit <http://creativecommons.org/licenses/by-nc-nd/4.0/>.

© The Author(s) 2025